

Structure and Width of the $d^*(2380)$ Dibaryon

Avraham Gal

Abstract In this contribution, dedicated to the memory of Walter Greiner, we discuss the structure and width of the recently established $d^*(2380)$ dibaryon, confronting the consequences of our Pion Assisted Dibaryons hadronic model with those of quark motivated calculations. In particular, the relatively small width $\Gamma_{d^*} \approx 70$ MeV favors hadronic structure for the $d^*(2380)$ dibaryon rather than a six-quark structure.

1 Walter Greiner: recollections

This contribution is dedicated to the memory of Walter Greiner whose wide-ranging interests included exotic phases of matter. My first physics encounter with Walter was in Fall 1983 in a joint physics symposium hosted by him, see Fig. 1.



Fig. 1 Participants of the Frankfurt–Jerusalem Symposium in Frankfurt, 1983. Walter Greiner is 3rd left on the 1st row. Eli Friedman is 5th right on the 2nd row. I'm missing in this photo.

Racah Institute of Physics, The Hebrew University, Jerusalem 91904, Israel
e-mail: avragal@savion.huji.ac.il

Greiner's wide-ranging interests included also superheavy elements, so it was quite natural for him to ask my good colleague Eli Friedman, a leading figure in exotic atoms, whether extrapolating pionic atoms to superheavy elements would shed light on a then-speculated pion condensation phase. Subsequently in 1984 Eli spent one month in Frankfurt at Greiner's invitation, concluding together with Gerhard Soff [1] that the strong-interaction π_{1s}^- repulsive energy shift known from light pionic atoms persists also in superheavy elements, as shown in Fig. 2-left, thereby ruling out pion condensation for large Z . However, quite surprisingly, they also found that $1s$ & $2p$ π^- atomic states in normal heavy elements up to $Z \approx 100$ have abnormally small widths of less than 1 MeV owing to the repulsive π -nucleus strong interaction within the nuclear volume. Hence 'deeply bound' states (DBS) in pionic atoms are experimentally resolvable, although they cannot be populated radiatively as in light pionic atoms because the absorption width in the higher $3d$ state exceeds its radiative width by almost two orders of magnitude, as shown in Fig. 2-right.

Friedman and Soff's 1985 prediction of DBS was repeated three years later by Toki and Yamazaki [3], who apparently were not aware of it, and verified experimentally in 1996 at GSI in a $(d, {}^3\text{He})$ reaction on ${}^{208}\text{Pb}$ [4]. Subsequent experiments on Pb and Sn isotopes have yielded accurate data on several other pionic-atom DBS [5], showing clear evidence in support of Weise's 1990 conjecture of partial chiral symmetry restoration in the nuclear medium due to a renormalized isovector s -wave πN interaction through the decrease of the pion-decay constant f_π [6]. However, the few DBS established so far are still short of providing on their own the precision reached by comprehensive fits to *all* (of order 100) pionic atom data, dominantly in higher atomic orbits, in substantiating this conjecture; for a recent review on the state of the art in pionic atoms see Ref. [7].

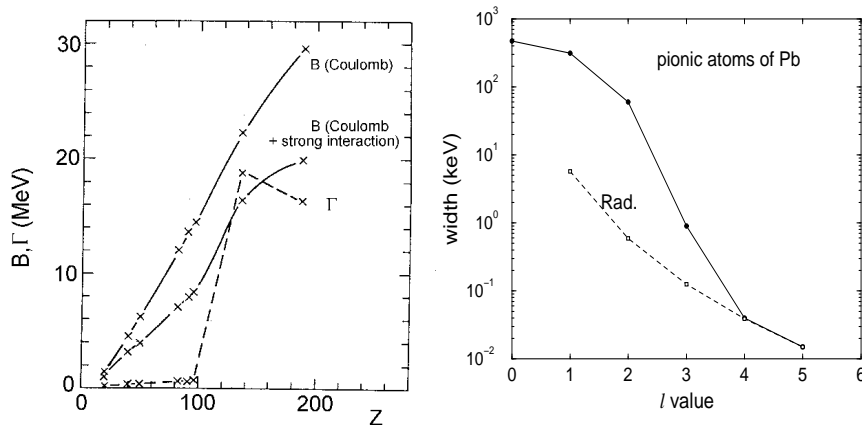


Fig. 2 First prediction of deeply bound pionic atom states [1]. The left panel shows binding energies and widths in $1s$ deeply bound pionic states [1], and the right panel shows the width saturation in circular states of pionic atoms of Pb [2].

My own encounters with Walter Greiner and several of his colleagues in Frankfurt during several Humboldt-Prize periods in the 1990s focused on developing the concept of Strange Hadronic Matter [8, 9, 10] and also on studying Kaon Condensation [11]. I recall fondly that period. Here I highlight another exotic phase of matter: non-strange Pion Assisted Dibaryons, reviewed by me recently in Ref. [12].

2 Pion assisted $N\Delta$ and $\Delta\Delta$ dibaryons

2.1 The Dyson-Xuong 1964 prediction

Non-strange s -wave dibaryon resonances \mathcal{D}_{IS} with isospin I and spin S were predicted by Dyson and Xuong in 1964 [13] as early as SU(6) symmetry proved successful, placing the nucleon $N(939)$ and its P_{33} πN resonance $\Delta(1232)$ in the same **56** multiplet. These authors chose the **490** lowest-dimension SU(6) multiplet in the 56×56 direct product containing the flavor-SU(3) $\overline{\mathbf{10}}$ and **27** multiplets in which the deuteron, \mathcal{D}_{01} , and NN virtual state, \mathcal{D}_{10} , are classified. Four more non-strange dibaryons emerged in this scheme, with masses listed in Table 1 in terms of constants A and B . Identifying A with the NN threshold mass 1878 MeV, the value $B \approx 47$ MeV was derived by assigning \mathcal{D}_{12} to the $pp \leftrightarrow \pi^+ d$ coupled-channel resonance behavior noted then at 2160 MeV, near the $N\Delta$ threshold (2.171 MeV). This led in particular to a predicted mass $M = 2350$ MeV for the $\Delta\Delta$ dibaryon candidate \mathcal{D}_{03} assigned at present to the recently established $d^*(2380)$ resonance [14].

Table 1 Predicted masses of non-strange $L = 0$ dibaryons \mathcal{D}_{IS} with isospin I and spin S , using the Dyson-Xuong SU(6) \rightarrow SU(4) mass formula $M = A + B[I(I+1) + S(S+1) - 2]$ [13].

\mathcal{D}_{IS}	\mathcal{D}_{01}	\mathcal{D}_{10}	\mathcal{D}_{12}	\mathcal{D}_{21}	\mathcal{D}_{03}	\mathcal{D}_{30}
BB'	NN	NN	$N\Delta$	$N\Delta$	$\Delta\Delta$	$\Delta\Delta$
SU(3) _f	$\overline{\mathbf{10}}$	27	27	35	$\overline{\mathbf{10}}$	28
$M(\mathcal{D}_{IS})$	A	A	$A + 6B$	$A + 6B$	$A + 10B$	$A + 10B$

In retrospect, the choice of the **490** lowest-dimension SU(6) multiplet, with Young tableau denoted [3,3,0], is not accidental. This [3,3,0] is the one adjoint to [2,2,2] for color-SU(3) singlet six-quark (6q) state, thereby ensuring a totally antisymmetric color-flavor-spin-space 6q wavefunction, assuming a totally symmetric $L = 0$ orbital component. For non-strange dibaryons, flavor-SU(3) reduces to isospin-SU(2), whence flavor-spin SU(6) reduces to isospin-spin SU(4) in which the [3,3,0] representation corresponds to a **50** dimensional representation consisting of precisely the I, S values of the dibaryon candidates listed in Table 1, as also noted recently in Ref. [15]. Since the **27** and $\overline{\mathbf{10}}$ flavor-SU(3) multiplets accommodate NN s -wave states that are close to binding (1S_0) or weakly bound (3S_1), we focus here on the \mathcal{D}_{12} and \mathcal{D}_{03} dibaryon candidates assigned to these flavor-SU(3) multiplets.

2.2 Pion assisted dibaryons

The pion plays a major role as a virtual particle in binding or almost binding NN s -wave states. The pion as a real particle interacts strongly with nucleons, giving rise to the $\pi N P_{33}$ p -wave $\Delta(1232)$ resonance. Can it also assist in binding two nucleons into s -wave $N\Delta$ states? And once we have such $N\Delta$ states, can the pion assist in binding them into s -wave $\Delta\Delta$ states? This is the idea behind the concept developed by Garcilazo and me of pion assisted dibaryons [16, 17], or more generally meson assisted dibaryons to go beyond the non-strange sector, see Ref. [12] for review.

As discussed in the next subsection, describing $N\Delta$ systems in terms of a stable nucleon (N) and a two-body πN resonance (Δ) leads to a well defined πNN three-body model in which $IJ = 12$ and 21 resonances identified with the \mathcal{D}_{12} and \mathcal{D}_{21} dibaryons of Table 1 are generated. This relationship between $N\Delta$ and πNN may be generalized into relationship between a two-body $B\Delta$ system and a three-body πNB system, where the baryon B stands for N, Δ, Y (hyperon) etc. In order to stay within a three-body formulation one needs to assume that the baryon B is stable. For $B = N$, this formulation relates the $N\Delta$ system to the three-body πNN system. For $B = \Delta$, once properly formulated, it relates the $\Delta\Delta$ system to the three-body $\pi N\Delta$ system, suggesting to seek $\Delta\Delta$ dibaryon resonances by solving $\pi N\Delta$ Faddeev equations, with a stable Δ . The decay width of the Δ resonance is considered then at the penultimate stage of the calculation. In terms of two-body isobars we have then a coupled-channel problem $B\Delta \leftrightarrow \pi D$, where D stands generically for appropriate dibaryon isobars: (i) \mathcal{D}_{01} and \mathcal{D}_{10} , which are the NN isobars identified with the deuteron and virtual state respectively, for $B = N$, and (ii) \mathcal{D}_{12} and \mathcal{D}_{21} for $B = \Delta$.

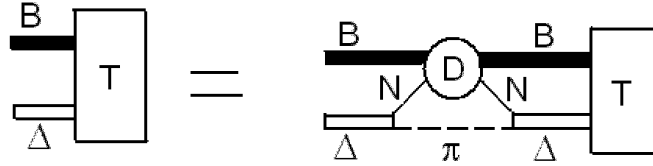


Fig. 3 Diagrammatic representation of the integral equation for the $B\Delta T$ matrix, derived by using separable pairwise interactions in πNB Faddeev equations [17] and solved numerically to calculate $B\Delta$ dibaryon resonance poles for $B = N, \Delta$.

Within this model, and using separable pairwise interactions, the coupled-channel $B\Delta - \pi D$ eigenvalue problem reduces to a single integral equation for the $B\Delta T$ matrix shown diagrammatically in Fig. 3, where starting with a $B\Delta$ configuration the Δ -resonance isobar decays into πN , followed by $NB \rightarrow NB$ scattering through the D -isobar with a spectator pion, and ultimately by means of the inverse decay $\pi N \rightarrow \Delta$ back into the $B\Delta$ configuration. We note that the interaction between the π meson and B is neglected for $B = \Delta$, for lack of known $\pi\Delta$ isobar resonances in the relevant energy range.

2.3 $N\Delta$ dibaryons

The \mathcal{D}_{12} dibaryon of Table 1 shows up clearly in the Argand diagram of the NN 1D_2 partial wave which is coupled above the $NN\pi$ threshold to the $I = 1$ s -wave $N\Delta$ channel. Values of \mathcal{D}_{12} and \mathcal{D}_{21} pole positions $W = M - i\Gamma/2$ from our hadronic-model three-body πNN Faddeev calculations [16, 17] described in the previous subsection are listed in Table 2 together with results of phenomenological studies that include (i) early NN phase shift analyses [18] and (ii) $pp \leftrightarrow np\pi^+$ coupled-channels analyses [19]. The \mathcal{D}_{12} mass and width values calculated in the Faddeev hadronic model version using $r_\Delta \approx 1.3$ fm are remarkably close to the phenomenologically derived ones, whereas the mass evaluated in the version using $r_\Delta \approx 0.9$ fm agrees with that assumed in the Dyson-Xuong pioneering discussion [13].

Table 2 \mathcal{D}_{12} and \mathcal{D}_{21} $N\Delta$ dibaryon S -matrix pole positions $W = M - i\frac{\Gamma}{2}$ (in MeV), obtained by solving the $N\Delta$ T -matrix integral equation of Fig. 3 [17], are listed for two choices of the $\pi N P_{33}$ form factor specified by a radius parameter r_Δ (in fm) together with two phenomenological values. The last column lists the results of a nonrelativistic meson-exchange Faddeev calculation.

$N\Delta$	Phenomenological		Faddeev (present)		Faddeev (non rel.)
\mathcal{D}_{1S}	Ref. [18]	Ref. [19]	$r_\Delta \approx 1.3$	$r_\Delta \approx 0.9$	Ref. [20]
\mathcal{D}_{12}	2148–i63	2144–i55	2147–i60	2159–i70	2116–i61
\mathcal{D}_{21}	–	–	2165–i64	2169–i69	–

Recent $pp \rightarrow pp\pi^+\pi^-$ production data [21] locate the \mathcal{D}_{21} dibaryon resonance almost degenerate with the \mathcal{D}_{12} . Our πNN Faddeev calculations produce it about 10-20 MeV higher than the \mathcal{D}_{12} , see Table 2. The widths of these near-threshold $N\Delta$ dibaryons are, naturally, close to that of the Δ resonance. We note that only 3S_1 NN enters the calculation of the \mathcal{D}_{12} resonance, while for the \mathcal{D}_{21} resonance calculation only 1S_0 NN enters, both with maximal strength. Obviously, with the 1S_0 interaction the weaker of the two, one expects indeed that the \mathcal{D}_{21} resonance lies above the \mathcal{D}_{12} resonance. Moreover, these two dibaryon resonances differ also in their flavor-SU(3) classification, see Table 1, which is likely to push up the \mathcal{D}_{21} further away from the \mathcal{D}_{12} . Finally, the $N\Delta$ s -wave states with $IJ = 11$ and 22 are found not to resonate in the πNN Faddeev calculations [17].

2.4 $\Delta\Delta$ dibaryons

The \mathcal{D}_{03} dibaryon of Table 1 shows up in the 3D_3 nucleon-nucleon partial wave above the $NN\pi\pi$ threshold owing to the coupling between the $I = 0$ 3D_3 NN channel and the $I = 0$ 7S_3 $\Delta\Delta$ channel, i.e. the coupling between the two-body NN channel and the four-body $NN\pi\pi$ channel. Indeed its best demonstration is by the relatively narrow peak about 80 MeV above the $\pi^0\pi^0$ production threshold and 80 MeV below the $\Delta\Delta$ threshold, with $\Gamma_{d^*} \approx 70$ MeV, observed in $pn \rightarrow d\pi^0\pi^0$ by the WASA-at-

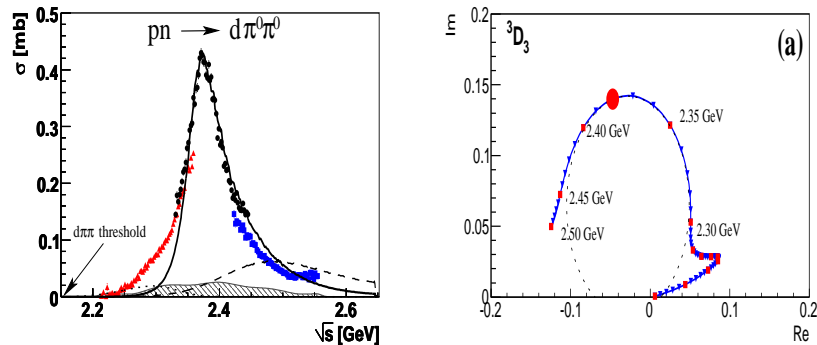


Fig. 4 $d^*(2380)$ dibaryon resonance signatures in recent WASA-at-COSY Collaboration experiments. Left: from the peak observed in the $pn \rightarrow d\pi^0\pi^0$ reaction [22]. Right: from the Argand diagram of the 3D_3 partial wave in pn scattering [23].

COSY Collaboration [22] and shown in Fig. 4-left. The $I = 0$ isospin assignment follows from the isospin balance in $pn \rightarrow d\pi^0\pi^0$, and the $J^P = 3^+$ spin-parity assignment follows from the measured deuteron angular distribution. The $d^*(2380)$ was also observed in $pn \rightarrow d\pi^+\pi^-$ [24], with cross section consistent with that measured in $pn \rightarrow d\pi^0\pi^0$, and studied in several $pn \rightarrow NN\pi\pi$ reactions [25, 26, 27]. Recent measurements of pn scattering and analyzing power [23] have led to the pn 3D_3 partial-wave Argand diagram shown in Fig. 4-right, supporting the \mathcal{D}_3 dibaryon resonance interpretation.

Table 3 \mathcal{D}_3 mass (in GeV) predicted in several quark-based calculations prior to 2008. Wherever calculated, the mass of \mathcal{D}_{12} is also listed.

\mathcal{D}_{1S} (BB')	[13]	[28]	[29]	[30]	[31]	[32]	[33]	[34]	exp./phen.
\mathcal{D}_{03} ($\Delta\Delta$)	2.35	2.36	2.46	2.42	2.38	≤ 2.26	2.40	2.46	2.38
\mathcal{D}_{12} ($N\Delta$)	2.16	2.36	-	-	2.36	-	-	2.17	≈ 2.15

The history and state of the art of the \mathcal{D}_3 dibaryon, now denoted $d^*(2380)$, were reviewed recently by Clement [14]. In particular, its mass was predicted in several quark-based calculations, as listed in Table 3 in the columns following the symmetry-based value predicted first by Dyson and Xuong [13]. Also listed are \mathcal{D}_{12} mass values, wherever available from such calculations. Remarkably, none of these quark-based predictions managed to reproduce the empirical mass values listed in the last column for *both* \mathcal{D}_{12} and \mathcal{D}_3 . More recent quark-based calculations, following the 2008 first announcement of observing the \mathcal{D}_3 [35], are discussed below.

Values of \mathcal{D}_3 and \mathcal{D}_{30} pole positions $W = M - i\Gamma/2$ from our hadronic-model three-body $\pi N\Delta$ Faddeev calculations [16, 17] are listed in Table 4. The \mathcal{D}_3 mass and width values calculated in the Faddeev hadronic model version using

$r_\Delta \approx 1.3$ fm are remarkably close to the experimentally reported ones, whereas the mass evaluated in the model version using $r_\Delta \approx 0.9$ fm agrees, perhaps fortuitously so, with that derived in the Dyson-Xuong pioneering discussion [13]. For smaller values of r_Δ one needs to introduce explicit vector-meson and/or quark-gluon degrees of freedom which are outside the scope of the present model. In contrast, the calculated widths Γ are determined primarily by the phase space available for decay, displaying little sensitivity to the radius r_Δ of the $\pi N P_{33}$ form factor.

Table 4 \mathcal{D}_{03} and \mathcal{D}_{30} $\Delta\Delta$ dibaryon S -matrix pole position $W = M - i\frac{\Gamma}{2}$ (in MeV), obtained in our hadronic model by solving the $\Delta\Delta$ T -matrix integral equation of Fig. 3, are listed for two choices of the $\pi N P_{33}$ form factor specified by a radius parameter r_Δ (in fm). The last two columns list results of post 2008 quark-based RGM calculations with hidden-color $\Delta_8\Delta_8$ components.

$\Delta\Delta$	Faddeev (present)		Recent quark-based	
	$r_\Delta \approx 1.3$	$r_\Delta \approx 0.9$	Ref. [36]	Ref. [37]
\mathcal{D}_{03}	2383-i41	2343-i24	2393-i75	2380-i36
\mathcal{D}_{30}	2411-i41	2370-i22	2440-i100	-

The \mathcal{D}_{30} dibaryon resonance is found in our $\pi N\Delta$ Faddeev calculations to lie about 30 MeV above the \mathcal{D}_{03} . These two states are degenerate in the limit of equal $D = \mathcal{D}_{12}$ and $D = \mathcal{D}_{21}$ isobar propagators in Fig. 3. Since \mathcal{D}_{12} was found to lie lower than \mathcal{D}_{21} , we expect also \mathcal{D}_{03} to lie lower than \mathcal{D}_{30} as satisfied in our Faddeev calculations. Moreover, here too the difference in their flavor-SU(3) classification will push the \mathcal{D}_{30} further apart from the \mathcal{D}_{03} . The \mathcal{D}_{30} has not been observed and only upper limits for its production in $pp \rightarrow pp\pi^+\pi^+\pi^-\pi^-$ are available [38].

Finally, we briefly discuss the \mathcal{D}_{03} mass and width values, listed in the last two columns of Table 4, from two recent quark-based resonating-group-method (RGM) calculations [36, 37] that add $\Delta_8\Delta_8$ hidden-color (CC) components to a $\Delta_1\Delta_1$ cluster. Interestingly, the authors of Ref. [36] have just questioned the applicability of admixing CC components in dibaryon calculations [39]. The two listed calculations generate mass values that are close to the mass of the $d^*(2380)$. The calculated widths, however, differ a lot from each other: one calculation generates a width of 150 MeV [36], exceeding substantially the reported value $\Gamma_{d^*(2380)} = 80 \pm 10$ MeV [23], the other one generates a width of 72 MeV [37], thereby reproducing the $d^*(2380)$ width. While the introduction of CC components has moderate effect on the resulting mass and width in the chiral version of the first calculation, lowering the mass by 20 MeV and the width by 25 MeV, it leads to substantial reduction of the width in the second (also chiral) calculation from 133 MeV to 72 MeV. The reason is that the dominant CC $\Delta_8\Delta_8$ components, with 68% weight [37], cannot decay through single-fermion transitions $\Delta_8 \rightarrow N_1\pi_1$ to asymptotically free color-singlet hadrons. However, as argued in the next section, these quark-based width calculations miss important kinematical ingredients that make the width of a single compact $\Delta_1\Delta_1$ cluster considerably smaller than $\Gamma_{d^*(2380)}$. The introduction of substantial $\Delta_8\Delta_8$ components only aggravates the disagreement.

3 The width of $d^*(2380)$, small or large?

The width derived for the $d^*(2380)$ dibaryon resonance by the WASA-at-COSY Collaboration and the SAID Data-Analysis-Center is $\Gamma_{d^*(2380)}=80\pm 10$ MeV [23]. It is much smaller than 230 MeV, twice the width $\Gamma_{\Delta} \approx 115$ MeV [40, 41] of a single free-space Δ , expected naively for a $\Delta\Delta$ quasibound configuration. However, considering the reduced phase space, $M_{\Delta} = 1232 \Rightarrow E_{\Delta} = 1232 - B_{\Delta\Delta}/2$ MeV in a bound- Δ decay, where $B_{\Delta\Delta} = 2 \times 1232 - 2380 = 84$ MeV is the $\Delta\Delta$ binding energy, the free-space Δ width gets reduced to 81 MeV using the in-medium single- Δ width $\Gamma_{\Delta \rightarrow N\pi}$ expression obtained from the empirical Δ -decay momentum dependence

$$\Gamma_{\Delta \rightarrow N\pi}(q_{\Delta \rightarrow N\pi}) = \gamma \frac{q_{\Delta \rightarrow N\pi}^3}{q_0^2 + q_{\Delta \rightarrow N\pi}^2}, \quad (1)$$

with $\gamma = 0.74$ and $q_0 = 159$ MeV [42]. Yet, this simple estimate is incomplete since neither of the two Δ s is at rest in a deeply bound $\Delta\Delta$ state. To take account of the $\Delta\Delta$ momentum distribution, we evaluate the bound- Δ decay width $\bar{\Gamma}_{\Delta \rightarrow N\pi}$ by averaging $\Gamma_{\Delta \rightarrow N\pi}(\sqrt{s_{\Delta}})$ over the $\Delta\Delta$ bound-state momentum-space distribution,

$$\bar{\Gamma}_{\Delta \rightarrow N\pi} \equiv \langle \Psi^*(p_{\Delta\Delta}) | \Gamma_{\Delta \rightarrow N\pi}(\sqrt{s_{\Delta}}) | \Psi(p_{\Delta\Delta}) \rangle \approx \Gamma_{\Delta \rightarrow N\pi}(\sqrt{\bar{s}_{\Delta}}), \quad (2)$$

where $\Psi(p_{\Delta\Delta})$ is the $\Delta\Delta$ momentum-space wavefunction and the dependence of $\Gamma_{\Delta \rightarrow N\pi}$ on $q_{\Delta \rightarrow N\pi}$ for on-mass-shell nucleons and pions was replaced by dependence on $\sqrt{s_{\Delta}}$. The averaged bound- Δ invariant energy squared \bar{s}_{Δ} is defined by

$$\bar{s}_{\Delta} = (1232 - B_{\Delta\Delta}/2)^2 - P_{\Delta\Delta}^2, \quad (3)$$

in terms of a $\Delta\Delta$ bound-state r.m.s. momentum $P_{\Delta\Delta} \equiv \langle p_{\Delta\Delta}^2 \rangle^{1/2}$.

Table 5 Values of $\sqrt{\bar{s}_{\Delta}}$, of the corresponding decay-pion momentum $\bar{q}_{\Delta \rightarrow N\pi}$ and of $\bar{\Gamma}_{\Delta \rightarrow N\pi}$ (2), listed as a function of $R_{\Delta\Delta}$ using $P_{\Delta\Delta}R_{\Delta\Delta} = \frac{3}{2}$ in Eq. (3). The last column lists deduced values of $\bar{\Gamma}_{\Delta\Delta \rightarrow NN\pi}$, approximating it by $\frac{5}{3}\bar{\Gamma}_{\Delta \rightarrow N\pi}$ (see text).

$R_{\Delta\Delta}$ (fm)	$\sqrt{\bar{s}_{\Delta}}$ (MeV)	$\bar{q}_{\Delta \rightarrow N\pi}$ (MeV)	$\bar{\Gamma}_{\Delta \rightarrow N\pi}$ (MeV)	$\bar{\Gamma}_{\Delta\Delta \rightarrow NN\pi}$ (MeV)
0.6	1083	38.3	1.6	2.6
0.7	1112	96.6	19.3	32.1
0.8	1131	122.0	33.5	55.8
1.0	1153	147.7	50.6	84.4
1.5	1174	170.4	67.4	112.3
2.0	1181	177.9	73.2	122.0

In Table 5, taken from my recent work [43], we list values of $\sqrt{\bar{s}_{\Delta}}$ and the associated in-medium decay-pion momentum $\bar{q}_{\Delta \rightarrow N\pi}$ for several representative values of the r.m.s. radius $R_{\Delta\Delta} \equiv \langle r_{\Delta\Delta}^2 \rangle^{1/2}$ of the bound $\Delta\Delta$ wavefunction, using the equality sign in the uncertainty relationship $P_{\Delta\Delta}R_{\Delta\Delta} \geq 3/2$. Listed also are values

of the in-medium single- Δ width $\bar{\Gamma}_{\Delta \rightarrow N\pi}$ obtained from Eq. (2). It is implicitly assumed here that the empirical momentum dependence (1) provides a good approximation also for off-mass-shell Δ s. Finally, The last column of the table lists values of $\bar{\Gamma}_{\Delta\Delta \rightarrow NN\pi\pi}$ obtained by multiplying $\bar{\Gamma}_{\Delta \rightarrow N\pi}$ by two, for the two Δ s, while applying to one of them the isospin projection factor $2/3$ introduced in the Gal-Garcilazo hadronic model [16, 17] to obey the quantum statistics requirements in the leading final $NN\pi\pi$ decay channels. The large spread of $\bar{\Gamma}_{\Delta\Delta \rightarrow NN\pi\pi}$ width values exhibited in the table, all of which are much smaller than the 162 MeV obtained by ignoring in Eq. (3) the bound-state momentum distribution, demonstrates the importance of momentum-dependent contributions. It is seen that a compact $d^*(2380)$ with r.m.s. radius $R_{\Delta\Delta}$ less than 0.8 fm is incompatible with the experimental value $\Gamma_{d^*(2380)} = 80 \pm 10$ MeV from WASA-at-COSY and SAID even upon adding a non-pionic partial width $\Gamma_{\Delta\Delta \rightarrow NN} \sim 10$ MeV [23].

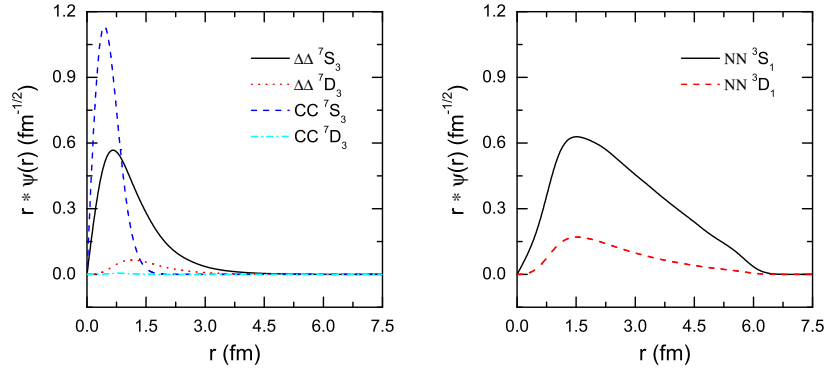


Fig. 5 $d^*(2380)$ $\Delta\Delta$ wavefunction with r.m.s. radius $R_{\Delta\Delta} = 0.76$ fm (Left) and deuteron wavefunction with r.m.s. radius $R_d \approx 2$ fm (Right) from recent quark-based RGM calculations [37, 44]. Figure adapted from Ref. [44].

Fig. 5 shows $d^*(2380)$ and $d(1876)$ wavefunctions from quark-based RGM calculations [37]. The $d^*(2380)$ appears quite squeezed compared to the diffuse deuteron. Its size, $R_{\Delta\Delta} = 0.76$ fm, leads to unacceptably small upper limit of about 47 MeV for the $d^*(2380)$ pionic width. This drastic effect of momentum dependence is missing in quark-based width calculations dealing with pionic decay modes of $\Delta_1\Delta_1$ components, e.g. Ref. [37]. Practitioners of quark-based models ought therefore to ask “what makes $\Gamma_{d^*(2380)}$ so much larger than the width calculated for a compact $\Delta\Delta$ dibaryon?” rather than “what makes $\Gamma_{d^*(2380)}$ so much smaller than twice a free-space Δ width?”

The preceding discussion of $\Gamma_{d^*(2380)}$ suggests that the quark-based model’s finding of a tightly bound $\Delta\Delta$ s -wave configuration is in conflict with the observed width. Fortunately, our hadronic-model calculations [16, 17] offer resolution of this

insufficiency by coupling to the tightly bound and compact $\Delta\Delta$ component of the $d^*(2380)$ dibaryon's wavefunction a $\pi N\Delta$ resonating component dominated asymptotically by a p -wave pion attached loosely to the near-threshold $N\Delta$ dibaryon \mathcal{D}_{12} with size about 1.5–2 fm. Formally, one can recouple spins and isospins in this $\pi\mathcal{D}_{12}$ system, so as to assume an extended $\Delta\Delta$ -like object. This explains why the preceding discussion of $\Gamma_{d^* \rightarrow NN\pi\pi}$ in terms of a $\Delta\Delta$ constituent model required a size larger than provided by quark-based RGM calculations [37] to reconcile with the reported value of $\Gamma_{d^*(2380)}$. We recall that the width calculated in our diffuse-structure $\pi N\Delta$ model [16, 17], as listed in Table 4, is in good agreement with the observed width of the $d^*(2380)$ dibaryon resonance.

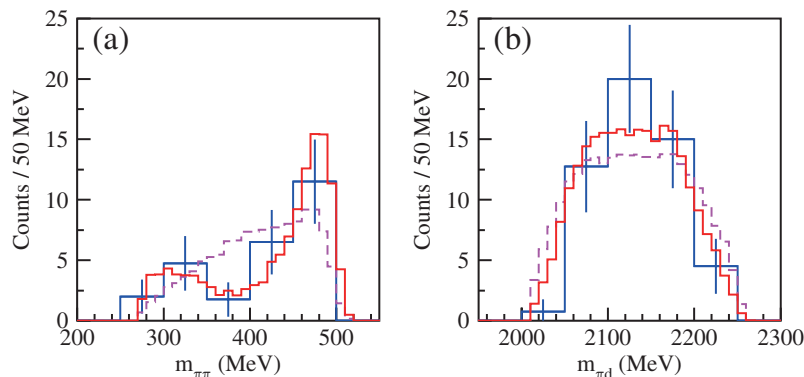


Fig. 6 Invariant mass distributions in ELPH experiment [45] $\gamma d \rightarrow d\pi^0\pi^0$ at $\sqrt{s} = 2.39$ GeV.

Support for the role of the $\pi\mathcal{D}_{12}$ configuration in the decay of the $d^*(2380)$ dibaryon resonance is provided by a recent ELPH $\gamma d \rightarrow d\pi^0\pi^0$ experiment [45] looking for the $d^*(2380)$. The cross section data agree with a relativistic Breit-Wigner resonance shape with mass of 2370 MeV and width of 68 MeV, but the statistical significance of the fit is low, particularly since most of the data are from the energy region above the $d^*(2380)$. Invariant mass distributions from this experiment at $\sqrt{s} = 2.39$ GeV, recorded in Fig. 6, are more illuminating. The $\pi\pi$ mass distribution shown in (a) suggests a two-bump structure, fitted in solid red. The lower bump around 300 MeV is perhaps a manifestation of the ABC effect [46], already observed in $pn \rightarrow d\pi^0\pi^0$ by WASA-at-COSY [22, 42] and interpreted in Ref. [43] as due to a tightly bound $\Delta\Delta$ decay with reduced $\Delta \rightarrow N\pi$ phase space. The upper bump in (a) is consistent then with the $d^*(2380) \rightarrow \pi\mathcal{D}_{12}$ decay mode, in agreement with the πd mass distribution shown in (b) that peaks slightly below the $\mathcal{D}_{12}(2150)$ mass.

Theoretical support for the relevance of the $\mathcal{D}_{12}(2150)$ $N\Delta$ dibaryon to the physics of the $d^*(2380)$ resonance is demonstrated in Fig. 7 [47] by showing a $d\pi$ invariant-mass distribution peaking near the $N\Delta$ threshold as deduced from the $pn \rightarrow d\pi^0\pi^0$ reaction by which the $d^*(2380)$ was found [22]. However, the peak is

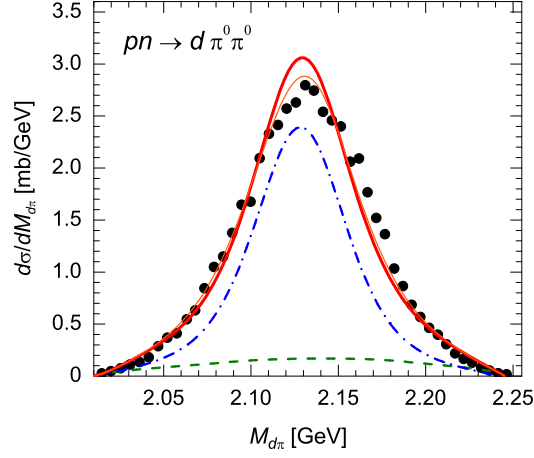


Fig. 7 The $pn \rightarrow d\pi^0\pi^0$ WASA-at-COSY $M_{d\pi}$ invariant-mass distribution [22] and, in solid lines, as calculated [47] for two input parametrizations of $\mathcal{D}_{12}(2150)$. The dot-dashed line gives the $\pi\mathcal{D}_{12}(2150)$ contribution to the two-body decay of the $d^*(2380)$ dibaryon, and the dashed line gives a σ -meson emission contribution. Figure adapted from Ref. [47].

shifted to about 20 MeV below the mass of the $\mathcal{D}_{12}(2150)$ and the width is smaller by about 40 MeV than the $\mathcal{D}_{12}(2150)$ width, agreeing perhaps fortuitously with $\Gamma_{d^*(2380)}$. Both of these features, the peak downward shift and the smaller width, can be explained by the asymmetry between the two emitted π^0 mesons, only one of which arises from the $\Delta \rightarrow N\pi$ decay within the $\mathcal{D}_{12}(2150)$ [47] (I am indebted to Heinz Clement for confirming to me this explanation).

Table 6 $d^*(2380)$ decay width branching ratios (BR in percents) from Ref. [43] for theory and from Refs. [48, 49] for experiment.

decay channel	$d\pi^0\pi^0$	$d\pi^+\pi^-$	$pn\pi^0\pi^0$	$pn\pi^+\pi^-$	$pp\pi^-\pi^0$	$nn\pi^+\pi^0$	$NN\pi$	NN	total
BR(th.)	11.2	20.4	11.6	25.8	4.7	4.7	8.3	13.3	100
BR(exp.)	14 ± 1	23 ± 2	12 ± 2	30 ± 5	6 ± 1	6 ± 1	≤ 9	12 ± 3	103

Recalling the $\Delta\Delta - \pi\mathcal{D}_{12}$ coupled channel nature of the $d^*(2380)$ in our hadronic model [16, 17], one may describe satisfactorily the $d^*(2380)$ total and partial decay widths in terms of an incoherent mixture of these relatively short-ranged ($\Delta\Delta$) and long-ranged ($\pi\mathcal{D}_{12}$) channels. This is demonstrated in Table 6 where the $NN\pi\pi$ calculated partial widths, totaling ≈ 60 MeV, are assigned a weight $\frac{5}{7}$ from $\Delta\Delta$ and a weight $\frac{2}{7}$ from $\pi\mathcal{D}_{12}$. This choice, ensuring that the partial decay width $\Gamma_{d^* \rightarrow NN\pi}$ does not exceed the upper limit of $\text{BR} \leq 9\%$ determined recently from *not* observing the single-pion decay branch [49], is by no means unique and the weights chosen here may be varied to some extent. For more details, see Ref. [43].

4 Conclusion

Substantiated by systematic production and decay studies in recent WASA-at-COSY experiments [14], the $d^*(2380)$ is the most spectacular dibaryon candidate at present. Following its early prediction in 1964 by Dyson and Xuong [13], it has been assigned in most theoretical works to a $\Delta\Delta$ quasibound state. Given the small width $\Gamma_{d^*(2380)} = 80 \pm 10$ MeV [23] with respect to twice the width of a free-space Δ , $\Gamma_\Delta \approx 115$ MeV, its location far from thresholds makes it easier to discard a possible underlying threshold effect. However, as argued in this review following Ref. [43], the observed small width is much larger than what two *deeply bound* Δ baryons can yield upon decay. The $d^*(2380)$ therefore cannot be described in terms of a single compact $\Delta\Delta$ state as quark-based calculations derive it [36, 37]. A complementary quasi two-body component is provided within a $\pi N\Delta$ three-body hadronic model [16, 17] by the $\pi\mathcal{D}_{12}$ channel, in which the $d^*(2380)$ resonates. The \mathcal{D}_{12} dibaryon stands here for the $I(J^P) = 1(2^+)$ $N\Delta$ near-threshold system that might possess a quasibound state S -matrix pole. It is a loose system of size 1.5–2 fm, as opposed to a compact $\Delta\Delta$ component of size 0.5–1 fm. It was also pointed out here, following Ref. [43], how the ABC low-mass enhancement in the $\pi^0\pi^0$ invariant mass distribution of the $pn \rightarrow d\pi^0\pi^0$ fusion reaction at $\sqrt{s} = 2.38$ GeV might be associated with a compact $\Delta\Delta$ component. The $\pi\mathcal{D}_{12}$ channel, in contrast, is responsible to the higher-mass structure of the $\pi^0\pi^0$ distribution and, furthermore, it gives rise to a non-negligible $d^* \rightarrow NN\pi$ single-pion decay branch, considerably higher than that obtained for a quark-based purely $\Delta\Delta$ configuration [50], but consistently with the upper limit of $\leq 9\%$ determined recently by the WASA-at-COSY Collaboration [49]. A precise measurement of this decay width and BR will provide a valuable constraint on the $\pi\mathcal{D}_{12}$ - $\Delta\Delta$ mixing parameter.

We end with a brief discussion of possible 6q admixtures in the essentially hadronic wavefunction of the $d^*(2380)$ dibaryon resonance. For this we refer to the recent 6q non-strange dibaryon variational calculation in Ref. [15] which depending on the assumed confinement potential generates a 3S_1 6q dibaryon about 550 to 700 MeV above the deuteron, and a 7S_3 6q dibaryon about 230 to 350 MeV above the $d^*(2380)$. Taking a typical 20 MeV potential matrix element from deuteron structure calculations and 600 MeV for the energy separation between the deuteron and the 3S_1 6q dibaryon, one finds admixture amplitude of order 0.03 and hence 6q admixture probability of order 0.001 which is compatible with that discussed recently by Miller [51]. Using the same 20 MeV potential matrix element for the $\Delta\Delta$ dibaryon candidate and 300 MeV for the energy separation between the $d^*(2380)$ and the 7S_3 6q dibaryon, one finds twice as large admixture amplitude and hence four times larger 6q admixture probability in the $d^*(2380)$, altogether smaller than 1%. These order-of-magnitude estimates demonstrate that long-range hadronic and short-range quark degrees of freedom hardly mix also for $\Delta\Delta$ configurations, and that the $d^*(2380)$ is extremely far from a pure 6q configuration. This conclusion is at odds with the conjecture made recently by Bashkanov, Brodsky and Clement [52] that 6q CC components dominate the wavefunctions of the $\Delta\Delta$ dibaryon candidates \mathcal{D}_{03} , identified with the observed $d^*(2380)$, and \mathcal{D}_{30} . Unfortunately, most of the

quark-based calculations discussed in the present work combine quark-model input with hadronic-exchange model input in a loose way which discards their predictive power.

Acknowledgements I'm indebted to the organizers of the Frontiers of Science symposium in memory of Walter Greiner, held at FIAS, Frankfurt, June 2017, particularly to Horst Stöcker, for inviting me to participate in this special event and for supporting my trip. Special thanks are due to Humberto Garcilazo, together with whom the concept of pion assisted dibaryons was conceived, and also due to Heinz Clement for many stimulating exchanges on the physics of dibaryons and Jerry Miller for instructive discussions on $6q$ contributions to dibaryons.

References

1. E. Friedman, G. Soff, *J. Phys. G* **11** (1985) L37.
2. E. Friedman, A. Gal, *Phys. Rep.* **452** (2007) 89.
3. H. Toki, T. Yamazaki, *Phys. Lett. B* **213** (1988) 129.
4. T. Yamazaki, R.S. Hayano, K. Itahashi, *et al.*, *Z. Phys. A* **355** (1996) 219.
5. T. Yamazaki, S. Hirenzaki, R.S. Hayano, H. Toki, *Phys. Rep.* **514** (2012) 1.
6. E.E. Kolomeitsev, N. Kaiser, W. Weise, *Phys. Rev. Lett.* **90** (2003) 092501, and references to earlier work by W. Weise listed therein.
7. E. Friedman, A. Gal, *Nucl. Phys. A* **928** (2014) 128, and references to earlier work listed therein.
8. J. Schaffner, C.B. Dover, A. Gal, C. Greiner, H. Stöcker, *Phys. Rev. Lett.* **71** (1993) 1328.
9. J. Schaffner, C.B. Dover, A. Gal, C. Greiner, D.J. Millener, H. Stöcker, *Ann. Phys.* **235** (1994) 35.
10. J. Schaffner-Bielich, A. Gal, *Phys. Rev. C* **62** (2000) 034311.
11. J. Schaffner, A. Gal, I.N. Mishustin, H. Stöcker, W. Greiner, *Phys. Lett. B* **334** (1994) 268.
12. A. Gal, *Acta Phys. Pol. B* **47** (2016) 471.
13. F.J. Dyson, N.-H. Xuong, *Phys. Rev. Lett.* **13** (1964) 815.
14. H. Clement, *Prog. Part. Nucl. Phys.* **93** (2017) 195.
15. W. Park, A. Park, S.H. Lee, *Phys. Rev. D* **92** (2015) 014037.
16. A. Gal, H. Garcilazo, *Phys. Rev. Lett.* **111** (2013) 172301.
17. A. Gal, H. Garcilazo, *Nucl. Phys. A* **928** (2014) 73.
18. R.A. Arndt, J.S. Hyslop III, L.D. Roper, *Phys. Rev. D* **35** (1987) 128, and references to earlier work listed therein.
19. N. Hoshizaki, *Phys. Rev. C* **45** (1992) R1424, *Prog. Theor. Phys.* **89** (1993) 563, and references to earlier work listed therein.
20. T. Ueda, *Phys. Lett. B* **119** (1982) 281.
21. P. Adlarson *et al.* (WASA-at-COSY Collaboration), arXiv:1803.03192-3.
22. P. Adlarson *et al.* (WASA-at-COSY Collaboration), *Phys. Rev. Lett.* **106** (2011) 242302.
23. P. Adlarson *et al.* (WASA-at-COSY Collaboration, SAID Data Analysis Center), *Phys. Rev. C* **90** (2014) 035204, and *Phys. Rev. Lett.* **112** (2014) 202301.
24. P. Adlarson *et al.* (WASA-at-COSY Collaboration), *Phys. Lett. B* **721** (2013) 229.
25. P. Adlarson *et al.* (WASA-at-COSY Collaboration), *Phys. Lett. B* **743** (2015) 325.
26. P. Adlarson *et al.* (WASA-at-COSY Collaboration), *Phys. Rev. C* **88** (2013) 055208.
27. G. Agakishiev *et al.*, *Phys. Lett. B* **750** (2015) 184.
28. P.J. Mulders, A.T. Aerts, J.J. de Swart, *Phys. Rev. D* **21** (1980) 2653.
29. M. Oka, K. Yazaki, *Phys. Lett. B* **90** (1980) 41.
30. M. Cvetič, B. Golli, N. Mankoč-Borštnik, M. Rosina, *Phys. Lett. B* **93** (1980) 489.
31. P.J. Mulders, A.W. Thomas, *J. Phys. G: Nucl. Part. Phys.* **9** (1983) 1159.

32. T. Goldman, K. Maltman, G.J. Stephenson, Jr., K.E. Schmidt, F. Wang, Phys. Rev. C **39** (1989) 1889.
33. X.Q. Zhang, Z.Y. Zhang, Y.W. Yu, P.N. Shen, Phys. Rev. C **60** (1999) 045203.
34. R.D. Mota, A. Valcarce, F. Fernandez, D.R. Entem, H. Garcilazo, Phys. Rev. C **65** (2002) 034006.
35. H. Clement *et al.* (CELSIUS-WASA Collaboration), Prog. Part. Nucl. Phys. **61** (2008) 276.
36. H. Huang, J. Ping, F. Wang, Phys. Rev. C **89** (2014) 034001, and references to earlier work listed therein.
37. Y. Dong, F. Huang, P. Shen, Z. Zhang, Phys. Rev. C **94** (2016) 014003, and references to earlier work listed therein.
38. P. Adlarson *et al.* (WASA-at-COSY Collaboration), Phys. Lett. B **762** (2016) 455.
39. F. Wang, J. Ping, H. Huang, arXiv:1711.01445v1.
40. R.A. Arndt, W.J. Briscoe, I.I. Strakovsky, R.L. Workman, Phys. Rev. C **76** (2007) 025209.
41. A.V. Anisovich, R. Beck, E. Klempt, V.A. Nikonov, A.V. Sarantsev, U. Thoma, Eur. Phys. J. A **48** (2012) 15.
42. M. Bashkanov, H. Clement, T. Skorodko, Nucl. Phys. A **958** (2017) 129.
43. A. Gal, Phys. Lett. B **769** (2017) 436.
44. F. Huang, Z.Y. Zhang, P.N. Shen, W.L. Wang, Chinese Phys. C **39** (2015) 071001, also available as arXiv:1408.0458v3 (nucl-th).
45. T. Ishikawa *et al.* (ELPH Experiment), Phys. Lett. B **772** (2017) 398.
46. A. Abashian, N.E. Booth, K.M. Crowe, Phys. Rev. Lett. **5** (1960) 258, substantiated by N.E. Booth, A. Abashian, K.M. Crowe, Phys. Rev. Lett. **7** (1961) 35.
47. M.N. Platonova, V.I. Kukulín, Nucl. Phys. A **946** (2016) 117.
48. M. Bashkanov, H. Clement, T. Skorodko, Eur. Phys. J. A **51** (2015) 87.
49. P. Adlarson *et al.* (WASA-at-COSY Collaboration), Phys. Lett. B **774** (2017) 559.
50. Y. Dong, F. Huang, P. Shen, Z. Zhang, Phys. Lett. B **769** (2017) 223.
51. G.A. Miller, Phys. Rev. C **89** (2014) 045203.
52. M. Bashkanov, S.J. Brodsky, H. Clement, Phys. Lett. B **727** (2013) 438.